ACS OMEGA

http://pubs.acs.org/journal/acsodf

Article

Numerical Study of a Capacitive Graphene Oxide Humidity Sensor with Etched Configuration

Meriam Mohammedture,* Shamma Al Hashmi, Jin-You Lu, Monserrat Gutierrez, Amal M. K. Esawi, and Mohamed Al Teneiji

Cite This: *ACS Omega* 2021, 6, 29781−29787

Read Online

ACCESS | Metrics & More | Article Recommendations

ABSTRACT: The geometrical dependence of humidity sensors on sensing performance has not been quantitatively outlined. Furthermore, the etching effect on humidity sensors is still elusive due to the difficulty in separating the effects of the geometrical change and etching-induced porosity on the overall performance. Here, we use COMSOL Multiphysics to perform a numerical study of a capacitive graphene oxide (GO) humidity sensor, with emphasis on the dimensions and etching effect on their sensing performance. GO is a useful and promising material in detecting humidity because of its selective superpermeability to water molecules. The mechanism of improved sensing performance of the etched humidity sensors is discussed in terms of the morphological profile and the effective permittivity including the etching-induced porosity effect. Our study shows that as compared to the unetched sensors, isotropic etching achieves the lowest response time of 1.011 s at 15.75% porosity, while vertical etching achieves the highest capacitance sensitivity of 0.106 fF/RH %.

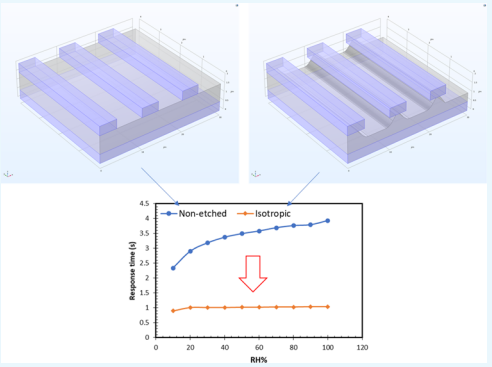

1. INTRODUCTION

Regulation and monitoring of humidity levels are increasingly becoming more important to instantly counteract any changes in the atmosphere that can affect the integrity of a system.[1,2] It can affect the health and safety of personnel, the cost of the product, and the manufacturing processes,[3,28] especially in agriculture[1,4] and medical monitoring.[5,6] A humidity sensor is an electronic device that measures the humidity in its environment and converts its findings into a corresponding electrical signal.[3] Considering the main types of sensors which are capacitive, resistive, surface acoustic waves, and optical, a capacitive-type sensor is chosen in this paper due to its ability to withstand drastic temperature and humidity changes, good stability and accuracy, and reproducible nature, making it a good option for humidity monitoring;[7−9] which is why it is the most commonly used type of sensor in the industry. A capacitive humidity sensor detects humidity due to a change in capacitance between two detection electrodes. This occurs due to the adsorption of water molecules by the sensing film which brings a change in the dielectric constant.[10]

The requirements a humidity sensor must meet are high sensitivity, rapid response and recovery time, small hysteresis, and good reproducibility. Several studies have been carried out to improve the sensing performance using advanced materials. The use of nanomaterials has greatly enhanced the sensing performance of humidity sensors, including exhibiting a wider humidity detection range, higher capacitance sensitivity, and improved response time.[11−13] However, since synthesis of the required nanomaterial involves complex processes, there has been interest in producing low-cost and easily manufactured sensors.[14,15] In addition to deploying new materials in the humidity sensor applications, morphological improvement has been another interest in this field. For instance, serpentine electrodes can achieve higher capacitance sensitivity compared to planar printed[16] or the empirical metallization ratio, $\eta = W/(W + G)$, indicates relationship between electrode finger width (W), spacing (G), and sensitivity of the sensor.[17]

More recently, a few studies have proposed adding the etching process to improve the sensing performance of the humidity sensor. Etching of the sensing material creates roughness in the surface, which results in the improvement of response time and capacitance sensitivity.[7,8,18] However, despite these studies, the mechanism of the etching effect on the humidity sensor is still elusive due to the difficulty in separating the effects of the geometrical change and etching-induced porosity on the overall performance.

Received: August 8, 2021
Accepted: October 15, 2021
Published: October 27, 2021

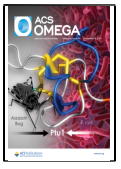

https://doi.org/10.1021/acsomega.1c04242
ACS Omega 2021, 6, 29781−29787

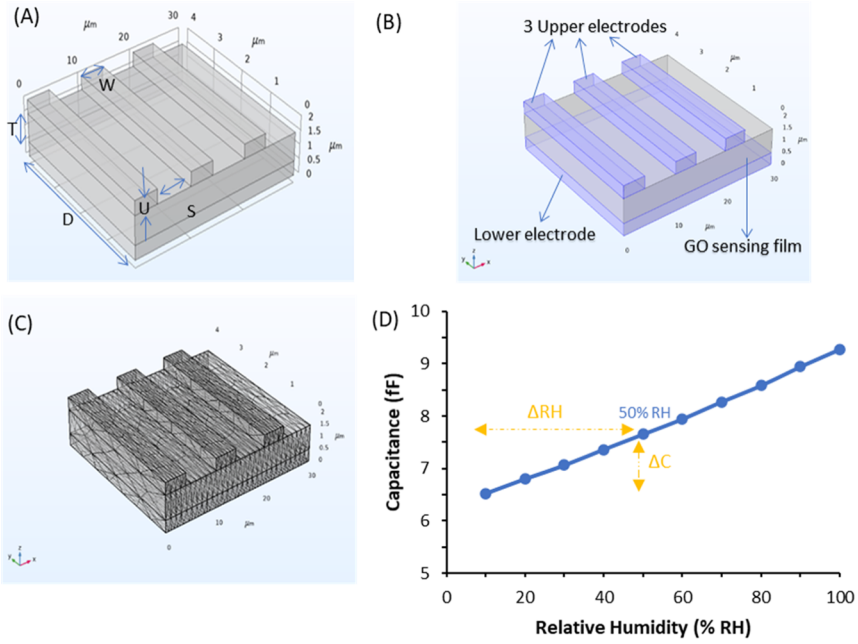

Figure 1. Modeled structure of the GO humidity sensors (A) parameters, (B) silver (Au) upper and lower electrodes and GO sensing film, (C) mesh analysis, and (D) capacitance variation of the humidity sensor with increasing RH from 10% RH to 100% RH under a constant measurement temperature of 25 °C, which is used to calculate sensitivity at a maximum of 50% RH.

In this work, we investigate the sensing properties of graphene oxide (GO) humidity sensors with a metal/insulator/metal configuration using COMSOL Multiphysics. GO is a great candidate as a sensing material due to its hydrophilic functional groups that enhance the adsorption of water molecules.[19] The aim was to determine how geometrical and morphological modifications affect the sensing properties of humidity sensors. The effect of geometrical dimensions on their sensing properties is first studied and can be a guideline to optimize the sensing performance of the humidity sensor. Then, the etched GO humidity sensors with different profiles, including isotropic, vertical, and directional etching, are considered to evaluate how the morphological change of the GO affects the overall performance. In addition, the effect of etching process-induced porosity in GO films is introduced by modifying its effective permittivity using the effective medium theory. We numerically demonstrate how the change of the geometrical dimension and porosity of the sensing film affect the performance of the humidity sensor, where the response times and capacitance sensitivity are compared and analyzed. Lastly, based on the simulation results, a novel etched configuration that produces optimized performance is proposed.

2. RESULTS AND DISCUSSION

To begin with a simple structure of the capacitive humidity sensors was designed, which consists of a lower electrode, three upper electrodes, and a sensing material sandwiched between the electrodes, as shown in Figure 1A,B. When running each model, the mesh size is defined as extra-fine, as seen in Figure 1C, and the temperature is set to 25 °C, which is the normal atmospheric temperature. The upper electrodes are parallel to each other with equal spacing in between the aligned bars to allow the permeation of water vapor through to the sensing film. Table 1 outlines the parameters that are defined in the modeling of the sensor.

Table 1. Structural Parameters of the Capacitive Humidity Sensor

Spacing between the upper electrodes (μm) S	Width of the upper electrodes (μm) W	Upper electrode thickness (μm) U	Thickness of the sensing film (μm) T	Depth (μm) D
6	4	0.5	1	4

Parameters such as response time and sensitivity are required when evaluating the performance of a sensor. The response time is defined as the time taken for the sensor's capacitance results to reach 90% of its final value starting from 0 s.[20] This was calculated from the capacitance versus time graph results analyzed at 50% relative humidity (RH).

The sensitivity is an important parameter when evaluating the performance of a humidity sensor. Sensitivity was calculated by taking the slope of the capacitance versus the RH curve, as shown in Figure 1D. This can also be expressed by the governing eq 1.

$$S = \frac{\Delta C}{\Delta \mathrm{RH}} = \frac{C_{50} - C_{10}}{50 - 10} (\mathrm{fF}/\%\ \mathrm{RH}) \quad (1)$$

here, ΔC denotes the difference between C_{50} and C_{10}, which are the capacitances corresponding to 50 and 10% RH, respectively. ΔRH denotes the difference between "50" and "10" values, which are the highest and lowest RH values taken to show the average sensitivity.[7,12,19,21]

2.1. Dimension Effect on the Sensor Performance. *2.1.1. Effect of Size of the Sensor.* The size of the sensor is becoming more important than ever in recent applications. Miniaturization of sensor devices offers many benefits such as low hysteresis and ease of packaging.[28] This was evaluated by decreasing the spacing between the electrodes, thickness, and width of the electrodes, the thickness of the sensing material, and the depth of the sensor by a factor of 2.

https://doi.org/10.1021/acsomega.1c04242
ACS Omega 2021, 6, 29781−29787

Figure 2 demonstrates a decrease in the response time as the size of the sensor is reduced. Upon decreasing the size of the

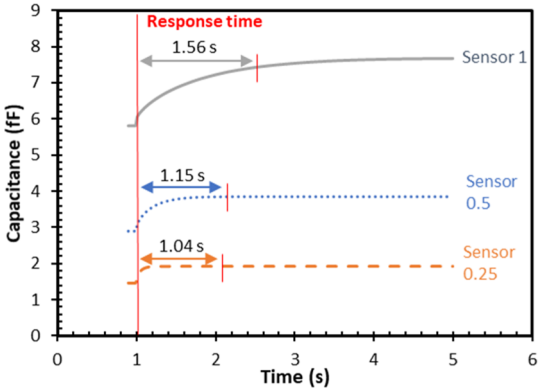

Figure 2. Capacitance vs time relationship of the humidity sensors at 50% RH upon decreasing the size by a factor of 2.

sensor by a factor of 2 from size 1 to 0.5, the response time decreases by 26%, delivering a final response time of 1.15 s, while the capacitance value decreases by half. This can be explained by the capacitance eq 2, where area is directly proportional to capacitance. By halving the size of the sensor, we are also halving the area of the sensing film and thus capacitance.

$$C = \frac{\varepsilon_r \varepsilon_o A}{d} \quad (2)$$

here, ε_r represents the relative permittivity of GO, ε_o is the permittivity of vacuum, A is the sensing area of the humidity sensor, and d is the thickness of the sensing layer.

It can be concluded that decreasing the size of the device improves the response time. This is because as the device becomes smaller, it takes less time for the water molecules to adsorb and diffuse into GO to reach saturation. Therefore, by decreasing this moisture adsorption path, the response of the sensor improves. This shows that if the width of the electrode is small and the total surface of the upper electrode is small, the absolute capacitance of the structure is small and thus sensitivity. Hence, the smaller the device, the more the sensor meets the conditions of fast response. However, fabrication limits intensify, and industrialization becomes difficult even if improvement in sensing performance is achieved.

2.1.2. Effect of Width of the Upper Electrode. Here, the effect of the width of the upper electrodes on sensing performance is investigated by decreasing the width in 1 μm step increments. Figure 3 shows that by decreasing the width of the upper electrode, the response time is improved. The humidity sensors with 1 μm width of upper electrodes displayed the shortest response time of 1.10 s at 50% RH. Accordingly, decreasing the upper electrode width by 1 μm steps improves the response time by an average of 10%. Hence, when we decrease the width of the electrode from 5 to 4 μm, the calculated response time decreases from 1.75 to 1.56 s, respectively.

This phenomenon can be supported by the fact that decreasing the width of the upper electrodes decreases the ratio between the electrode width (W) and the spacing (S) between the upper electrodes (W/S). The response time is proportional to the W/S ratio, as seen in Figure 3. Hence, the smaller the width, the faster the response of the sensor.

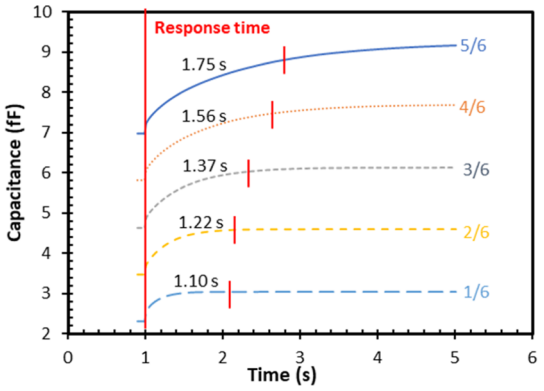

Figure 3. Capacitance vs time relationship at 50% RH of the sensors when decreasing the width.

Furthermore, as the electrode width becomes smaller, the length to which water molecules diffuse in the covered parts (under the parallel electrodes) shortens, improving the response. The diffusion in the upper electrodes is a limiting phenomenon for the response time.[6]

2.1.3. Effect of Spacing between the Upper Electrodes. The spacing between the upper electrodes have been varied with a 1 μm step decrease starting from 6 μm. A final response time at 6 μm spacing achieved 1.56 s. Figure 4 shows that as

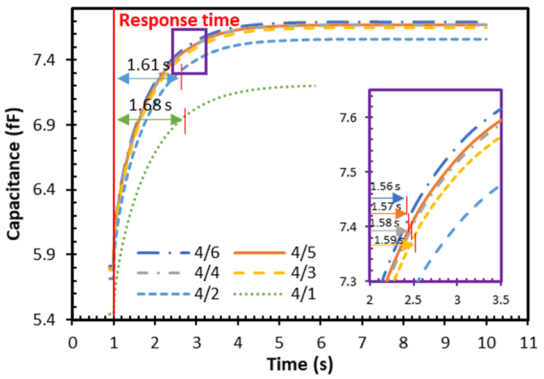

Figure 4. Capacitance vs time relationship at 50% RH of the sensor when decreasing the spacing between the upper electrodes by 1 μm.

the spacing between the upper electrodes increases and the W/S ratio decreases, the response time also decreases. Hence, by either increasing the spacing or decreasing the electrode width, the uncovered area of the sensing film increases. Thus, the contact area and rate of diffusion of water vapor in the sensing film increase, meeting the requirements of both high sensitivity and fast response.[6,22−24]

2.1.4. Varying the Thickness of the Sensing Film (Active Material). The thickness of the sensing film was varied from 1 to 2 μm to investigate the effect of film thickness on the response time and sensitivity. Figure 5 demonstrates that as the thickness of the GO film is reduced, the response time improves. Therefore, on decreasing the thickness of the sensing film by 0.25 μm steps starting from 2 μm thickness, the response time is improved by 4%. The fastest response time of 1.56 s is achieved when the thickness of the sensing film is equal to 1 μm. Decreasing the thickness of the sensing film shortens the diffusion length of the water vapor molecules in the sensing material, hence improving the response time.[24] Capacitance also decreases with increasing thickness, which is

https://doi.org/10.1021/acsomega.1c04242
ACS Omega 2021, 6, 29781−29787

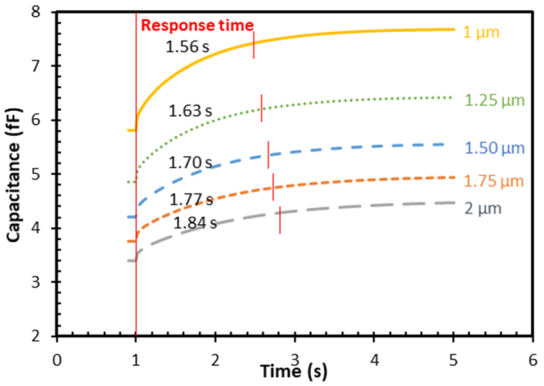

Figure 5. Capacitance vs time relationship at 50% RH of the sensor upon decreasing the thickness of GO film by 1 μm.

supported by governing eq 5. Furthermore, as expected, thickness of the sensing film is a limiting phenomenon for affordable humidity sensors since fabrication methods must be kept in mind as it becomes more difficult at a smaller scale. Therefore, 1 μm was chosen as the appropriate sensing film thickness as any value lower than this will result in a more complex deposition process.

2.2. Etching of the Sensing Material. *2.2.1. Three Different Etched Configurations.* The effect of etched configuration on the response time and sensitivity of the humidity sensor was studied. Three types of etched configurations are introduced, which are the isotropic, directional, and vertical etch. Isotropic etching is usually achieved by the chemical (wet) etching process, and the directional and vertical etching are achieved by the physical dry etching process.[25] The response time and sensitivity of novel etched configurations were modeled to compare their sensing performance with non-etched sensors, which has an average response time of 1.56s and a sensitivity of 3.76×10^{-2} fF/RH %, as shown in Table 1. The isotropically etched humidity sensor configuration comprises etching of the sensing area between the upper electrodes, as shown in Figure 6A. The calculated response time is equal to 1.01 s, and sensitivity is equal to 2.80×10^{-2} fF/RH %. The areas between the upper electrodes were directionally etched, as shown in Figure 6B, resulting in a response time of 1.03 s and a sensitivity of 2.85×10^{-2} fF/RH %. Lastly, as seen in Figure 6C, the area between the electrodes was vertically etched, resulting in a response time of 1.04 s and a sensitivity of 5.32×10^{-2} fF/RH %.

Figure 6D shows that the decrease in response time of the etched device is due to the shortening of the moisture adsorption path and the increased contact area of the uncovered sensing material.[8,26] Since the sensitivity is approximately proportional to the sensing material area, by removing some of the sensing material during the etching process, sensitivity is presumed to decrease. However, experimentally, capacitance sensitivity increases.[7] By comparing the response time of each sensor (isotropic, vertical, directional, and nonetched) at each RH as shown in Figure 6D,E, it is seen that the among three different etched profiles, the isotropically etched sensor has the lowest response time.

2.2.2. Porosity Effect Resulting from Etching. In addition to the change of the morphologies of the sensing material, the porosity resulting from the etching process is discussed in this section. We discussed three different etching conditions included in the porosity in the Landau–Lifshitz–Looyenga (LLL) effective medium model. For unetched GO, the fitted porosity of permittivity of the GO is 11.5%. To include the increased porosity, three different etched porosity rates with the values of 8.5, 17, and 25.5% per 1 μm etching depth are considered. The effective permittivity fitted using the LLL model with the 11.5% porosity is called the permittivity of the intrinsic (unetched) GO, and the effective permittivity fitted

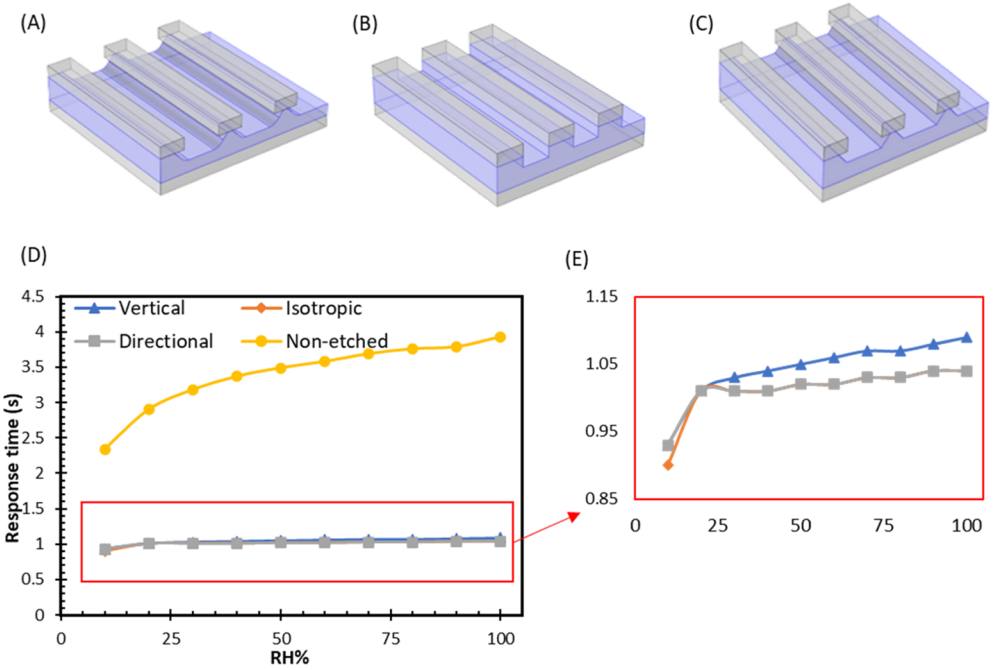

Figure 6. Etched configuration. (A) Isotropic, (B) directional, (C) vertical. (D) Response time variation taken at each RH of the different etched configurations before and after adding 15.75% change in porosity to the model. (E) Magnified section of the overlapped etched configurations variation from the graph (D) of response time taken at each RH.

https://doi.org/10.1021/acsomega.1c04242
ACS Omega 2021, 6, 29781−29787

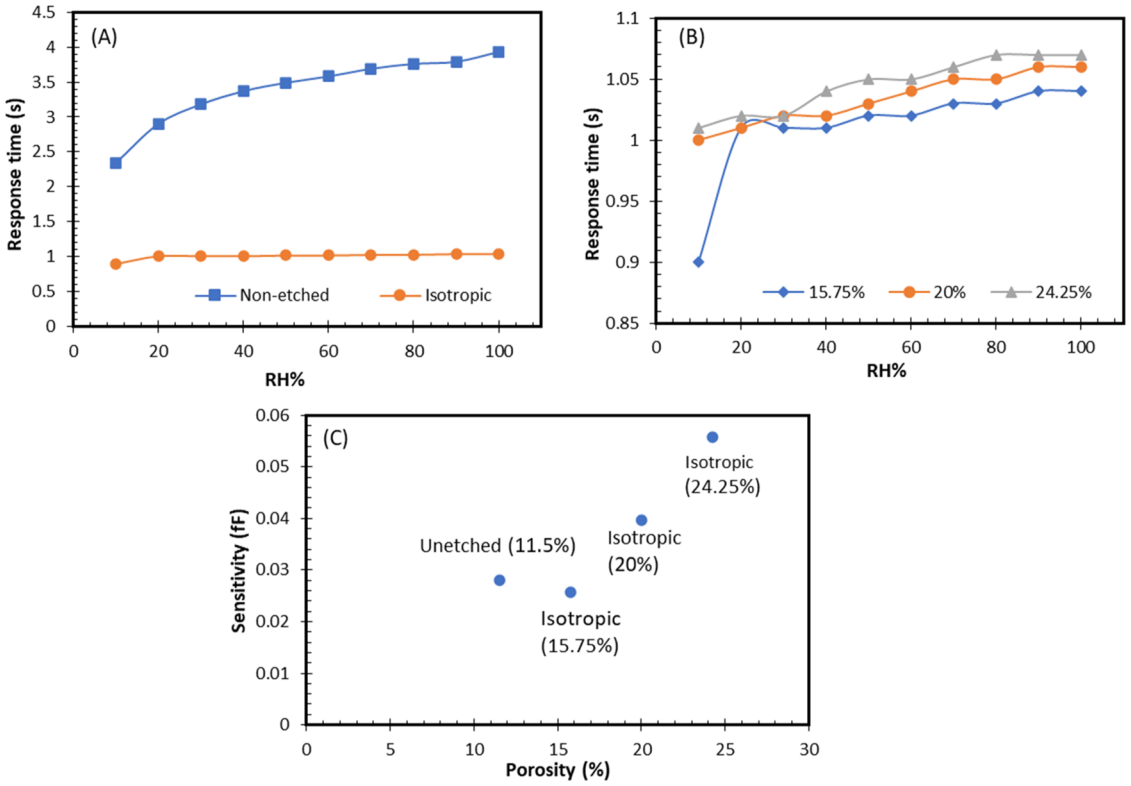

Figure 7. (A) Response time as a function of RH % of nonetched and isotropically etched humidity sensor with 15.75% porosity, (B) response time as a function of RH % of isotropic etching with 15.75, 20, and 24.25% porosity, (C) sensitivity as a function of porosity of the unetched and isotropically etched humidity sensor, where the change in the capacitance is calculated from that at 50% to 10% RH.

with higher porosities is called the permittivity of the etched graphene.

The fitted permittivity of the etched GO is inputted into COMSOL simulation to evaluate how the porosity affects the response time and capacitance of the humidity sensors. Figure 7A shows the response time of unetched and isotropically etched humidity sensors, where the porosity effect is included in the effective permittivity of the etched GO. As compared to the simulation results in Figure 6D, the change in the porosity does not significantly affect the response time of the etched humidity sensors at different RH values; however, the morphology does. Figure 7B shows a comparison of isotropically etched humidity sensors with different porosities of 15.75, 20, and 24.25%, and the response time slightly increases with increasing porosity of GO as the diffusion constant of GO is assumed to be independent of its porosity.

Figure 7C shows the capacitance sensitivity of the unetched and isotropically etched humidity sensors. We can find that the increased porosity can improve the sensitivity of the humidity sensors, and it should be noted that the morphological change could possibly reduce the capacitance sensitivity due to the reduction of the capacitance. Considering the porosity in the effective permittivity of the sensing material, the predicted capacitance sensitivity agrees with the experimental observation.[8] Table 2 summarizes the capacitance sensitivity of different etched humidity sensors, including isotropic, directional, and vertical configurations. The simulation results show that isotropical etching is a superior option to achieve the fastest-response-time humidity sensor, while the vertical etching achieves the best-sensitivity humidity sensor.

Table 2. Response Time and Sensitivity of the Etched Humidity Sensor with Different Porosity Percentages, Where the Capacitance Sensitivity Is Calculated from That at 50% of the RH to 10% of the RH

	Isotropic	Directional	Vertical
Porosity percentage 11.4% (intrinsic GO)			
Response time (s)	1.136	1.136	1.275
Sensitivity (fF/RH %)	0.0280	0.0285	0.0532
Porosity percentage 15.75%			
Response time (s)	1.011	1.014	1.043
Sensitivity (fF/RH %)	0.0257	0.0259	0.0488
Porosity percentage 20%			
Response time (s)	1.034	1.034	1.07
Sensitivity (fF/RH %)	0.0397	0.0401	0.0755
Porosity percentage 24.25%			
Response time (s)	1.046	1.046	1.087
Sensitivity (fF/RH %)	0.0557	0.0563	0.106

3. NUMERICAL METHOD

The simulation was done by using COMSOL Multiphysics 5.5. The simulation is based on the following assumptions: diffusion of water molecules in the film follows Henry's Law and Fick's Law. The humidity sensing mechanism is based on the change of the dielectric permittivity of the GO sensing film at different humidity values.[27] The water diffusion through the sensing material is studied using a finite element method implemented in the Transport of Dilute Species COMSOL module. The governing equation is given by eq 3

$$\frac{\partial c}{\partial t} + \nabla \cdot \vec{J} = R \qquad \vec{J} = -D\nabla c \tag{3}$$

https://doi.org/10.1021/acsomega.1c04242
ACS Omega 2021, 6, 29781−29787

where c is the concentration, J is the total flux, D is the diffusion constant of water in the sensing material, and R is the net water source. In this study, R is equal to zero. The capacitance of the humidity sensor is studied using the electrostatics COMSOL module. The governing equation is Poisson's equation, as given by eq 4

$$\nabla \cdot \vec{D} = \rho \qquad \vec{E} = -\nabla V \tag{4}$$

where V is the electrical potential and D and E are the electric displacement and electric field, respectively. The upper electrode is the applied voltage with the terminal boundary condition, while the lower electrode is grounded.

The dielectric constant of GO at different RH values was obtained from the experimental data presented in the previous literature.[28] The diffusion constant of GO was taken as 6.5×10^{-7} m^2/s.[29] To investigate the humidity sensing performance, the device was simulated at various levels of RH %. The values of RH were defined in COMSOL in the form of water vapor concentration c using an empirical eq 5, where "t" is equal to $1-373.15/T$ and T is the ambient temperature.[30]

$$c = \exp[13.3185t - 1.976t^2 - 0.6445t^3 - 0.1299t^4] \tag{5}$$

Using the concentration value "c" in eq 6, the water vapor concentration at each RH can be calculated.

$$wvc_{(\mathrm{mol}/m^3)} = \frac{\mathrm{RH}\ \% \times c}{18} \tag{6}$$

During the etching process, there is a relationship among the porosity of the sensing material, etching time, and material-etched depth, and it varies with the etching recipe and the materials. In general, the etching depth and the porosity are approximately linearly proportional to the etching time as the etching depth is few micrometers in range.[31,32] For instance, the porosity of porous silicon increases by 8.5% per 1 μm etching depth. To our best knowledge, this relationship is not presented in literature and highly depends on the etching parameter. Therefore, to generally consider the change of the porosity on GO resulting from the etching process, three different etching-induced porosity rates of 8.5, 17, and 25.5% per 1 μm etching depth are discussed.

The effect permittivity of GO can be calculated using the LLL effective medium theory[33,34] by incorporating the porosity into the model, as given by eq 7.

$$f_1\left(\frac{\varepsilon_1 - \varepsilon}{\varepsilon_1 + 2\varepsilon}\right) + f_2\left(\frac{\varepsilon_2 - \varepsilon}{\varepsilon_2 + 2\varepsilon}\right) + f_3\left(\frac{\varepsilon_3 - \varepsilon}{\varepsilon_3 + 2\varepsilon}\right) = 0 \tag{7}$$

where ε_1, ε_2, and ε_3 are the permittivities of air, water, and GO, respectively, and f_1, f_2, and f_3 are volume fractions of air, water, and GO, respectively. The initial volume fractions of 11.5, 0, and 88.5% are fitted with the experimentally measured permittivity of the unetched GO at different RHs.[28] Four different effective permittivities of the etched GO (etching depth of 0.4 μm) are shown in Figure 8.

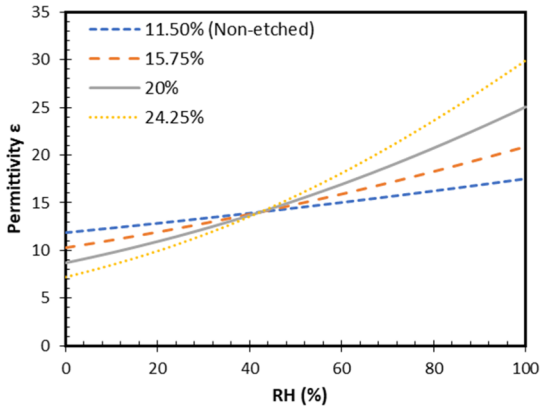

Figure 8. Investigation of the change in relative permittivity of the GO humidity sensor with different porosities resulting from different etching rates.

4. CONCLUSIONS

Investigating the geometrical dependence of humidity sensors has shown that optimizing the sensing material is not enough to accurately achieve the most optimal sensing performance. Here, we demonstrated the modeling and simulation of GO humidity sensors using COMSOL Multiphysics comparing different parameters and etching configurations. Regarding the GO capacitive humidity sensor, it is seen that some geometrical parameters such as decreasing the width of upper electrodes and increasing the spacing between upper electrodes improves the response time more than the other parameters. The simulation results show that isotropical etching shows the best improvement in the response time, while vertical etching shows highest sensitivity improvement. The vertically etched sensors presented here have a consistent increased sensitivity at different porosities, which indicates stable response of the device at low and high humidity levels and the highest sensitivity improvement.

AUTHOR INFORMATION

Corresponding Author

Meriam Mohammedture − *Nanomaterials Department, Advanced Materials Research Centre, Technology Innovation Institute, Abu Dhabi 9639, United Arab Emirates;* orcid.org/0000-0002-7030-438X;
Phone: +971589440990;
Email: Meriam.mohammedture@tii.ae

Authors

Shamma Al Hashmi − *Nanomaterials Department, Advanced Materials Research Centre, Technology Innovation Institute, Abu Dhabi 9639, United Arab Emirates*

Jin-You Lu − *Nanomaterials Department, Advanced Materials Research Centre, Technology Innovation Institute, Abu Dhabi 9639, United Arab Emirates*

Monserrat Gutierrez − *Nanomaterials Department, Advanced Materials Research Centre, Technology Innovation Institute, Abu Dhabi 9639, United Arab Emirates*

Amal M. K. Esawi − *Department of Mechanical Engineering, School of Sciences and Engineering, The American University in Cairo, New Cairo 11835, Egypt;* orcid.org/0000-0001-9515-400X

Mohamed Al Teneiji − *Nanomaterials Department, Advanced Materials Research Centre, Technology Innovation Institute, Abu Dhabi 9639, United Arab Emirates*

Complete contact information is available at: https://pubs.acs.org/10.1021/acsomega.1c04242

Notes

The authors declare no competing financial interest.

https://doi.org/10.1021/acsomega.1c04242
ACS Omega 2021, 6, 29781−29787

■ ACKNOWLEDGMENTS

The authors thank the support from other members in the Advanced Materials Research Centre at Technology Innovation Institute and thank the Abu Dhabi Government's Advanced Technology Research Council (ATRC), which oversees technology research in the Emirates.

■ REFERENCES

(1) Park, D.-H.; Park, J.-W. Wireless Sensor Network-Based Greenhouse Environment Monitoring and Automatic Control System for Dew Condensation Prevention. *Sensors* **2011**, *11*, 3640−3651.
(2) Jia, Y.; Heiß, M.; Fu, Q.; Gay, N. A. A Prototype RFID Humidity Sensor for Built Environment Monitoring. *2008 International Workshop on Education Technology and Training and 2008 International Workshop on Geoscience and Remote Sensing*, 2008; Vol. 2, pp 496−499. DOI: 10.1109/ettandgrs.2008.35
(3) Lee, C.-Y.; Lee, G.-B. Humidity Sensors: A Review. *Sens. Lett.* **2005**, *3*, 1−15.
(4) Adiono, T.; Fathany, M. Y.; Fuada, S.; Purwanda, I. G.; Anindya, S. F. A Portable Node of Humidity and Temperature Sensor for Indoor Environment Monitoring. *International Conference on Intelligent Green Building and Smart Grid* 2018; pp 1−5.
(5) Mitani, Y.; Miyaji, K.; Kaneko, S.; Uekura, T.; Momose, H.; Johguchi, K. A Compact Perspiration Meter System with Capacitive Humidity Sensor for Wearable Health-Care Applications. *Jpn. J. Appl. Phys.* **2018**, *57*, 04FF10.
(6) Tetelin, A.; Pellet, C. Modeling and Optimization of a Fast Response Capacitive Humidity Sensor. *IEEE Sens. J.* **2006**, *6*, 714−720.
(7) Qiang, T.; Wang, C.; Liu, M.-Q.; Adhikari, K. K.; Liang, J.-G.; Wang, L.; Li, Y.; Wu, Y.-M.; Yang, G.-H.; Meng, F.-Y.; Fu, J.-H.; Wu, Q.; Kim, N.-Y.; Yao, Z. High-Performance Porous MIM-Type Capacitive Humidity Sensor Realized via Inductive Coupled Plasma and Reactive-Ion Etching. *Sens. Actuators, B* **2018**, *258*, 704−714.
(8) Kim, J.-H.; Hong, S.-M.; Moon, B.-M.; Kim, K. High-Performance Capacitive Humidity Sensor with Novel Electrode and Polyimide Layer Based on MEMS Technology. *Microsyst. Technol.* **2010**, *16*, 2017−2021.
(9) Gu, L.; Huang, Q. A.; Qin, M. A Novel Capacitive-Type Humidity Sensor Using CMOS Fabrication Technology. *Sens. Actuators, B* **2004**, *99*, 491−498.
(10) Wang, J.; Wang, X.-h.; Wang, X.-d. Study on Dielectric Properties of Humidity Sensing Nanometer Materials. *Sens. Actuators, B* **2005**, *108*, 445−449.
(11) Qi, R.; Zhang, T.; Guan, X.; Dai, J.; Liu, S.; Zhao, H.; Fei, T. Capacitive Humidity Sensors Based on Mesoporous Silica and Poly(3,4-Ethylenedioxythiophene) Composites. *J. Colloid Interface Sci.* **2020**, *565*, 592−600.
(12) Pongampai, S.; Pengpad, P.; Meananeatra, R.; Chaisriratanakul, W.; Poyai, A.; Horprathum, M.; Chananonnawathorn, C.; Titiroongruang, W.; Muanghlua, R. Sensing Layer Combination of Vertically Aligned ZnO Nanorods and Graphene Oxide for Ultrahigh Sensitivity IDE Capacitive Humidity Sensor. *IEEJ Trans. Electr. Electron. Eng.* **2020**, *15*, 965−975.
(13) Duan, Z.-H.; Zhao, Q.-N.; Li, C.-Z.; Wang, S.; Jiang, Y.-D.; Zhang, Y.-J.; Liu, B.-H.; Tai, H.-L. Enhanced Positive Humidity Sensitive Behavior of P-Reduced Graphene Oxide Decorated with n-WS2 Nanoparticles. *Rare Met.* **2021**, *40*, 1762−1767.
(14) Duan, Z.; Zhao, Q.; Wang, S.; Huang, Q.; Yuan, Z.; Zhang, Y.; Jiang, Y.; Tai, H. Halloysite nanotubes: Natural, environmental-friendly and low-cost nanomaterials for high-performance humidity sensor. *Sensor* **2020**, *317*, 128204.
(15) Duan, Z.; Jiang, Y.; Zhao, Q.; Wang, S.; Yuan, Z.; Zhang, Y.; Liu, B.; Tai, H. Facile and Low-Cost Fabrication of a Humidity Sensor Using Naturally Available Sepiolite Nanofibers. *Nanotechnology* **2020**, *31*, 355501.
(16) Rivadeneyra, A.; Fernández-Salmerón, J.; Agudo-Acemel, M.; López-Villanueva, J. A.; Capitan-Vallvey, L. F.; Palma, A. J. Printed Electrodes Structures as Capacitive Humidity Sensors: A Comparison. *Sens. Actuators, A* **2016**, *244*, 56−65.
(17) Oikonomou, P.; Patsis, G. P.; Botsialas, A.; Manoli, K.; Goustouridis, D.; Pantazis, N. A.; Kavadias, A.; Valamontes, E.; Ganetsos, T.; Sanopoulou, M.; Raptis, I. Performance Simulation, Realization and Evaluation of Capacitive Sensor Arrays for the Real Time Detection of Volatile Organic Compounds. *Microelectron. Eng.* **2011**, *88*, 2359−2363.
(18) Zhou, W.; He, X.; Wu, J.; Wang, L.; Wang, L. Numerical Study on Response Time of a Parallel Plate Capacitive Polyimide Humidity Sensor Based on Microhole Upper Electrode. *J. Micro/Nanolithogr., MEMS, MOEMS* **2017**, *16*, 034502.
(19) Guo, R.; Tang, W.; Shen, C.; Wang, X. High Sensitivity and Fast Response Graphene Oxide Capacitive Humidity Sensor with Computer-Aided Design. *Comput. Mater. Sci.* **2016**, *111*, 289−293.
(20) Bi, H.; Yin, K.; Xie, X.; Ji, J.; Wan, S.; Sun, L.; Terrones, M.; Dresselhaus, M. S. Ultrahigh Humidity Sensitivity of Graphene Oxide. *Sci. Rep.* **2013**, *3*, 2714.
(21) Alrammouz, R.; Podlecki, J.; Vena, A.; Garcia, R.; Abboud, P.; Habchi, R.; Sorli, B. Highly Porous and Flexible Capacitive Humidity Sensor Based on Self-Assembled Graphene Oxide Sheets on a Paper Substrate. *Sens. Actuators, B* **2019**, *298*, 126892.
(22) Benmoussa, N.; Benichou, A.; Medjahdi, N.; Rahmoun, K. Modeling and Optimization of a Capacitive Humidity Sensor Response in MEMS Technology. *Dielectr. Mater. Photovolt. Syst.* **2014**, 13−16.
(23) Karthick, R.; Babu, D. S.; Abirami, A.; Kalainila, S. Design of High Sensitivity and Fast Response MEMS Capacitive Humidity Sensor Using COMSOL Multiphysics. *Proceedings COMSOL Conference*, 2011.
(24) Zhou, W.-H.; Wang, L.-C.; Wang, L.-B. Numerical Study of the Structural Parameter Effects on the Dynamic Characteristics of a Polyimide Film Micro-Capacitive Humidity Sensor. *IEEE Sens. J.* **2016**, *16*, 5979−5986.
(25) Plummer, J. D.; Deal, M.; Griffin, P. B. *Silicon VLSI Technology: Fundamentals, Practice and Modeling*; Pearson College Div, 2000.
(26) Tételin, A.; Pellet, C.; Laville, C.; N'Kaoua, G. Fast Response Humidity Sensors for a Medical Microsystem. *Sens. Actuators, B* **2003**, *91*, 211−218.
(27) Farahani, H.; Wagiran, R.; Hamidon, M. Humidity Sensors Principle, Mechanism, and Fabrication Technologies: A Comprehensive Review. *Sensors* **2014**, *14*, 7881−7939.
(28) Huang, X.; Leng, T.; Georgiou, T.; Abraham, J.; Raveendran Nair, R.; Novoselov, K. S.; Hu, Z. Graphene Oxide Dielectric Permittivity at GHz and Its Applications for Wireless Humidity Sensing. *Sci. Rep.* **2018**, *8*, 43.
(29) Cho, Y. H.; Kim, H. W.; Lee, H. D.; Shin, J. E.; Yoo, B. M.; Park, H. B. Water and Ion Sorption, Diffusion, and Transport in Graphene Oxide Membranes Revisited. *J. Memb. Sci.* **2017**, *544*, 425−435.
(30) McRae, G. J. A Simple Procedure for Calculating Atmospheric Water Vapor Concentration. *J. Air Pollut. Control Assoc.* **1980**, *30*, 394.
(31) Behzad, K.; Yunus, W. M. M.; Talib, Z. A.; Zakaria, A.; Bahrami, A. Effect of Preparation Parameters on Physical, Thermal and Optical Properties of n-Type Porous Silicon. *Int. J. Electrochem. Sci.* **2012**, *7*, 8266−8275.
(32) Hadi, H. A. Modification of Surface Properties of Silicon Wafers by Laser-Assisted Electrochemical Etching. *Int. Lett. Chem. Phys. Astron.* **2018**, *80*, 30−39.
(33) Nazarov, R.; Zhang, T.; Khodzitsky, M. Effective Medium Theory for Multi-Component Materials Based on Iterative Method. *Photonics* **2020**, *7*, 113.
(34) Lu, J. Y.; Raza, A.; Fang, N. X.; Chen, G.; Zhang, T. Effective Dielectric Constants and Spectral Density Analysis of Plasmonic Nanocomposites. *J. Appl. Phys.* **2016**, *120*, 163103.